Supporting Information

Ultrahigh toughness of stretchable ratiometric mechano-fluorescent polyurethane elastomers enhanced by dual slide-ring motion of polyrotaxane cross-linkers and daisy chain backbones

Tu Thi Kim Cuc,[a] Yun-Chen Tso,[a] Ting-Chi Wu,[a] Pham Quoc Nhien,[b] Trang Manh Khang,[a] Bui Thi Buu Hue,[b] Wei-Tsung Chuang[c] and Hong-Cheu Lin*[a, d]

[a] Department of Materials Science and Engineering, National Yang Ming Chiao Tung University, Hsinchu 300093, Taiwan

[b] Department of Chemistry, College of Natural Sciences, Can Tho University, Can Tho City 94000, Viet Nam

[c] National Synchrotron Radiation Research Center, Hsinchu 300092, Taiwan

[d] Center for Emergent Functional Matter Science, National Yang Ming Chiao Tung University, Hsinchu 300093, Taiwan

1. General information

1.1 Materials

All necessary chemical reagents were purchased from commercial supplier sources of Sigma-Aldrich, Alfa Aesar, Combi Blocks, TCI, etc., and directly used without further purification. All solvents were dried/purified by the solvent purification system before applying for reactions. All reactions were proceeded under nitrogen gas and vacuum-line manipulations. Several chemicals and solvents with their abbreviations are listed as follows: *di-tert*-butyldicarbonate (Boc_2O), 4-dimethylaminopyridine (DMAP), 1,8-biazabicyclo[5.4.0] undec-7-ene (DBU), dibutyltin dilaurate (DBTDL), 1-ethyl-3-(3-dimethylaminopropyl) carbodiimide hydrochloride (EDC), ethylenediamine tetraacetic acid disodium salt dihydrate ($Na_2EDTA.2H_2O$), hexamethylene diisocyanate (HDI), triethanolamine (TEA), tetra-ethylene glycol (TEG), trifluoroacetic acid (TFA), *p*-toluenesulfonyl chloride (TsCl), dichloromethane (DCM), *N*,*N*-dimethylformamide (DMF), ethanol (EtOH), ethyl acetate (EtOAc), hexane (Hex), methanol (MeOH), tetrahydrofuran (THF) and acetonitrile (MeCN).

1.2 Instruments

Nuclear magnetic resonance (NMR) spectra were collected from Agilent 400-MR DD2, Varian Unity Inova 500 MHz, and Varian VNMRS-600 NMR spectrometers operating at frequencies of 400, 500 and 600 MHz at room temperature to verify chemical structures of all synthetic compounds. High resolution mass spectra (HRMS) were recorded on a Bruker-Impact HD Mass Spectrometer by using an electrospray ionization (ESI) technique. The fluorescence emission and absorbance spectra of all acquired compounds were obtained by using a Fluorescence Spectrophotometer (HITACHI F-7000) and an Ultraviolet-Visible Near-Infrared Spectrophotometer (Lambda 950, PerkinElmer), respectively. The fluorescence lifetime values of major compounds were gained from the time-resolved photoluminescence (TRPL) profiles revealed on a PDL 200 Pulsed Diode Laser. Fourier transform infrared spectroscopy (FTIR) PerkinElmer spectrum 100 was employed to analyze target samples at room temperature by 16 scan times from 4000 to 400 cm^{-1} with a bandwidth of 4 cm^{-1}. The mechanical properties of polymer films were evaluated by MTS Tytron 250 tensile system, and the thermal stability tests were examined by thermo-gravimetric analysis (TA instruments Q500, heating rate = 10 °C/min). Differential scanning calorimetry (DSC) profiles were obtained on a NETZSCH DSC under liquid nitrogen at a heating/cooling rate of 10 °C/min. The weights of all used materials were determined by a Mettler Toledo AG245 Analytical Balance. X-ray diffraction experiments including small-angle X-ray

scattering (SAXS) and wide-angle X-ray scattering (WAXS) measurements were performed on TPS 13A and TLS 17A beamlines at the National Synchrotron Radiation Research Center (NSRRC) in Hsinchu, Taiwan.

1.3 Mechanical testing

A MTS Tytron 250 tensile system was employed to record all stress-strain curves. The polymer films with the dog-bone shaped specimens were prepared. The middle sections of the dog-bone specimens were 5 mm in width and 10 mm in length. The thicknesses of the samples were identified by a micrometer, which varied from 0.4 mm to 0.5 mm. Before carrying out tensile strength tests, sample pieces were put on the jigs of the tension machine with an initial length of 1 mm, considered as the gap between two clips.

2. Experimental section

2.1 Synthetic routes

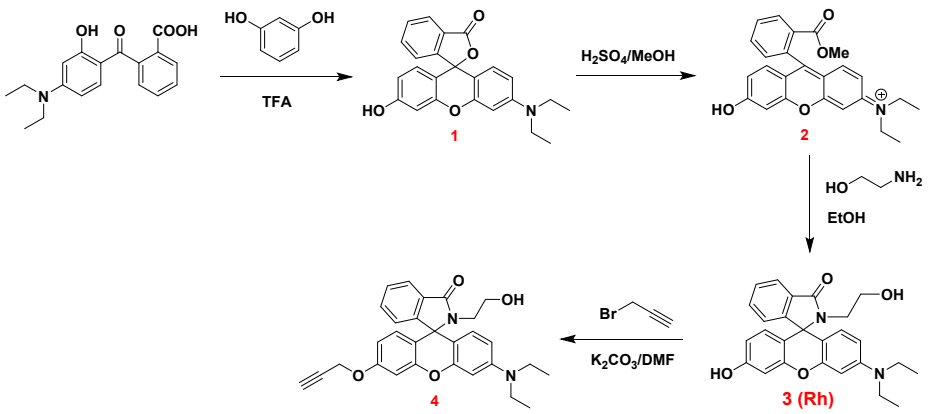

Scheme S1 Synthetic routes of rhodamine derivatives.

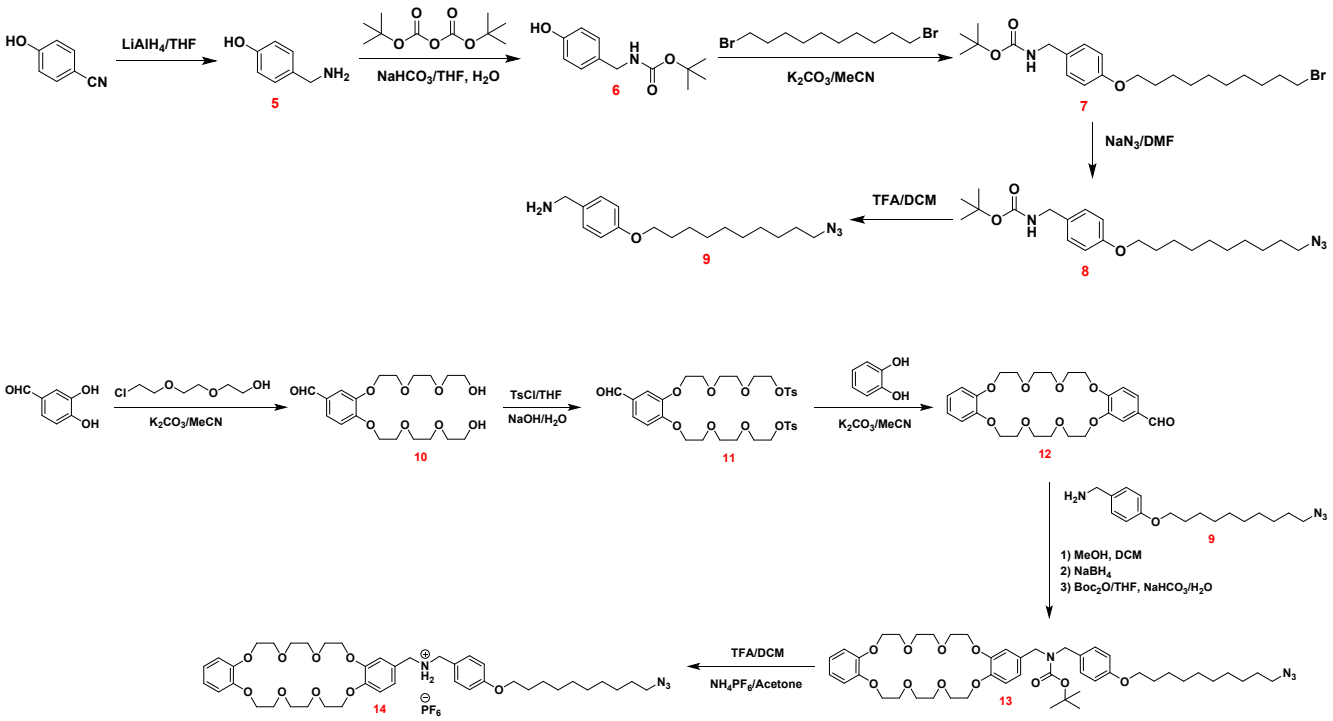

Scheme S2 Synthetic routes of alkyne **9** and DB24C8 wheel-appending secondary ammonium unit **14**.

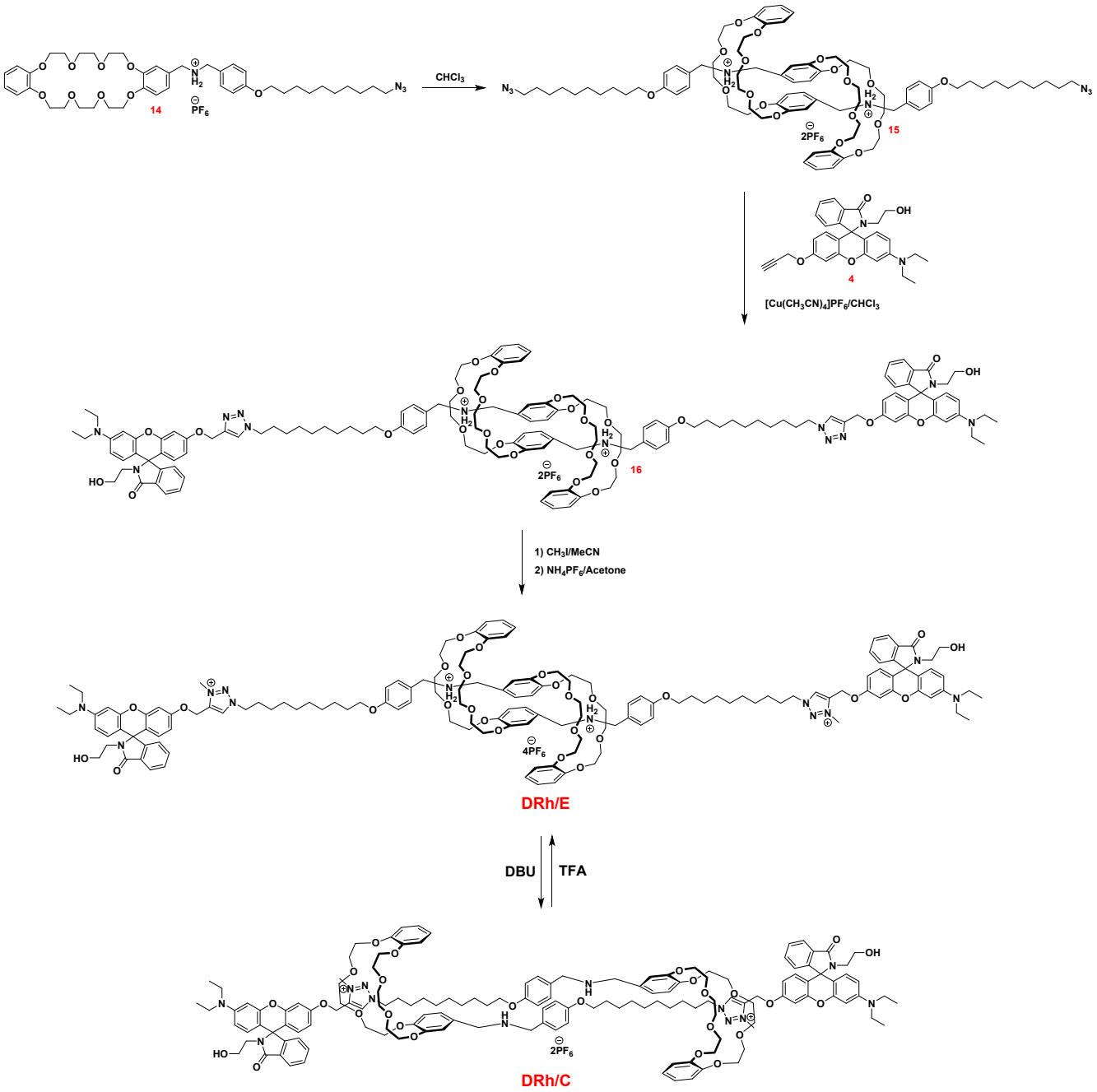

Scheme S3 Synthetic routes of daisy chain rotaxanes **DRh/E** and **DRh/C**.

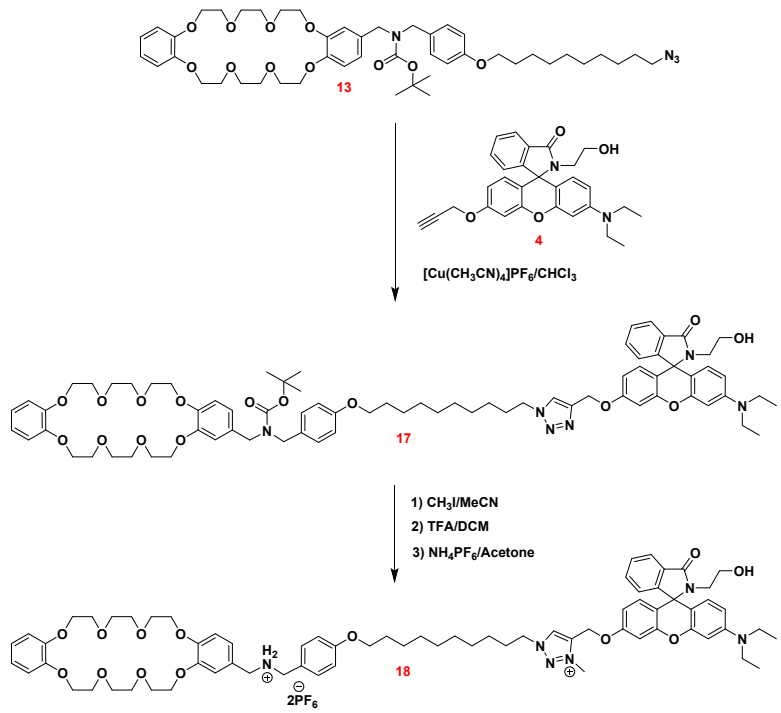

Scheme S4 Synthetic routes of non-interlocked analogue **18**.

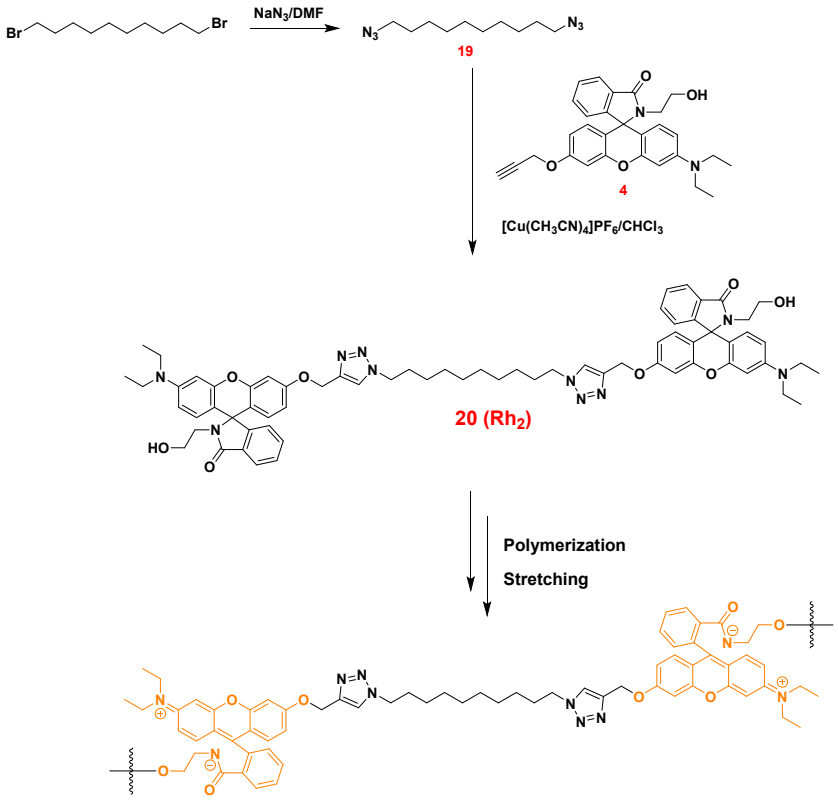

Scheme S5 Synthetic routes of bis-rhodamine derivative **20** (**Rh_2**).

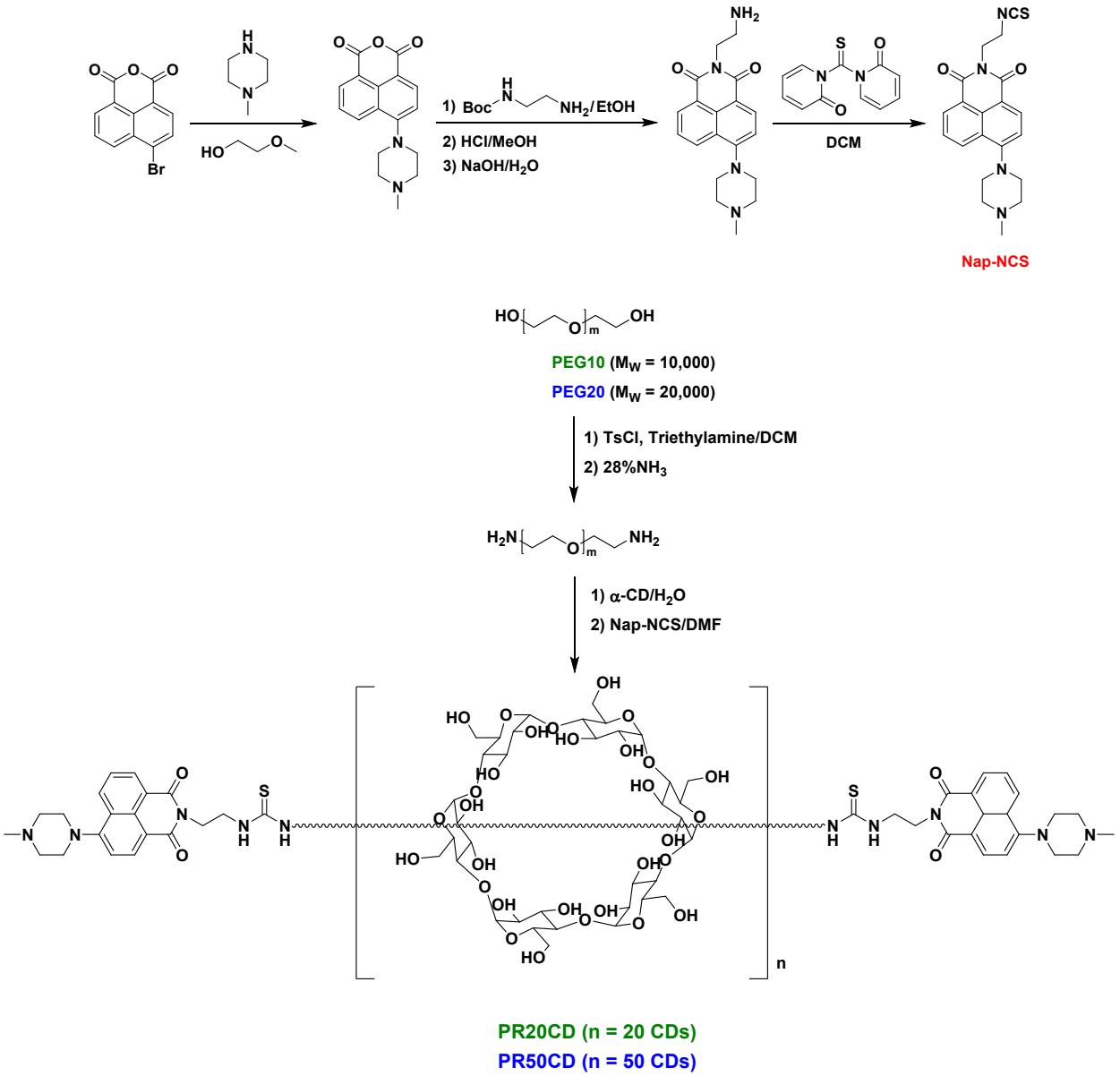

Scheme S6 Synthetic routes of polyrotaxanes **PR20CD** and **PR50CD**.

2.2 Synthetic procedures and characterizations of [c2] daisy chain rotaxane DRh/E and all related compounds

Compounds **1-3** were synthesized according to the previous publication with some modifications.[S1]

Compounds **5-11** was produced according to our previous publication.[S2]

Compounds **4**, **12-14**, **16-20** and **DRh/E** were generated according to our previous publication.[S3]

Synthesis of compound Nap-NCS: Compound **Nap-NCS** was synthesized according to our previous publication.[S4] ^{1}H NMR (400 MHz, $CDCl_3$, δ ppm): 8.59 (dd, J = 7.6 Hz, J = 1.2 Hz, 1H); 8.52 (d, J = 8.0 Hz, 1H); 8.42 (dd, J = 8.4 Hz, J = 1.2 Hz, 1H); 7.69 (dd, J = 8.4 Hz, J = 7.2 Hz, 1H);

7.22 (d, J = 8.4 Hz, 1H); 4.49 (t, J = 6.4 Hz, 2H); 3.89 (t, J = 6.4 Hz, 2H); 3.32 (t, J = 4.8 Hz, 4H); 2.76 (t, J = 4.8 Hz, 4H); 2.45 (s, 3H). ^{13}C NMR (125 MHz, $CDCl_3$, δ ppm): 164.48, 163.90, 156.43, 133.20, 132.06, 131.68, 130.90, 130.14, 126.26, 125.84, 122.81, 116.13, 115.22, 55.12, 52.92, 46.10, 42.97, 39.00, 32.02, 31.52, 30.26, 30.04, 29.79, 29.46, 22.79, 14.23.

Synthesis of compounds PR20CD and PR50CD: Compounds **PR20CD** and **PR50CD** were synthesized according to our previous publication.[S4]

PR20CD: ^{1}H NMR (600 MHz, DMSO-d_6, δ ppm): 8.47-8.41 (m, 6H); 7.80 (s, 2H); 7.33 (s, 2H); 5.65-5.64 (m, 115H); 5.50-5.41 (m, 103H); 4.77 (s, 111H); 4.42 (s, 121H); 3.72-3.26 (br); 2.29 (s, 6H). ^{13}C NMR (150 MHz, DMSO-d_6, δ ppm): 102.47, 82.51, 82.11, 73.78, 73.69, 72.57, 71.96, 70.22, 69.83, 59.97, 56.26, 55.08, 52.97, 46.18, 30.03.

PR50CD: ^{1}H NMR (600 MHz, DMSO-d_6, δ ppm): 8.39 (s, 6H); 7.78 (s, 2H); 7.32 (s, 2H); 5.64 (s, 285H); 5.47 (s, 305H); 4.75 (s, 291H); 4.43 (s, 302H); 3.69-3.24 (br); 2.27 (s, 6H). ^{13}C NMR (150 MHz, DMSO-d_6, δ ppm): 102.41, 82.51, 82.17, 73.82, 73.69, 72.56, 72.05, 70.22, 69.95, 60.41, 59.97, 31.14.

Preparation of PU films: All PU films were prepared according to the description in previous publications with some modifications.[S1,S4] Take the sample **PURh(s)** as a model. Compound **Rh** (21.5 mg, 0.05 mmol), tetraethylene glycol (TEG) (864.3 mg, 4.45 mmol), and dibutyltin dilaurate (DBTDL) (1 drop) were dissolved in dry THF (6 mL) was refluxed under N_2 atmosphere for 15 min. Then, hexamethylene diisocyanate (HDI) (1010.2 mg, 6.0 mmol) was added and the resultant mixture was continuously reacted for 1 h. Later on, a solution of triethanolamine (TEA) (37.3 mg, 0.25 mmol) in dry THF (2 mL) was further added in the above mixture solution and nonstop reacted for further 15 min. Subsequently, the resultant solution was poured into a Teflon coated model and dried in a vacuum oven at 70 °C for 1 day to gain a transparent straw-colored film.

Preparation of compound DRh/C: Compound **DRh/C** was prepared according to our previous publication.[S3,S5]

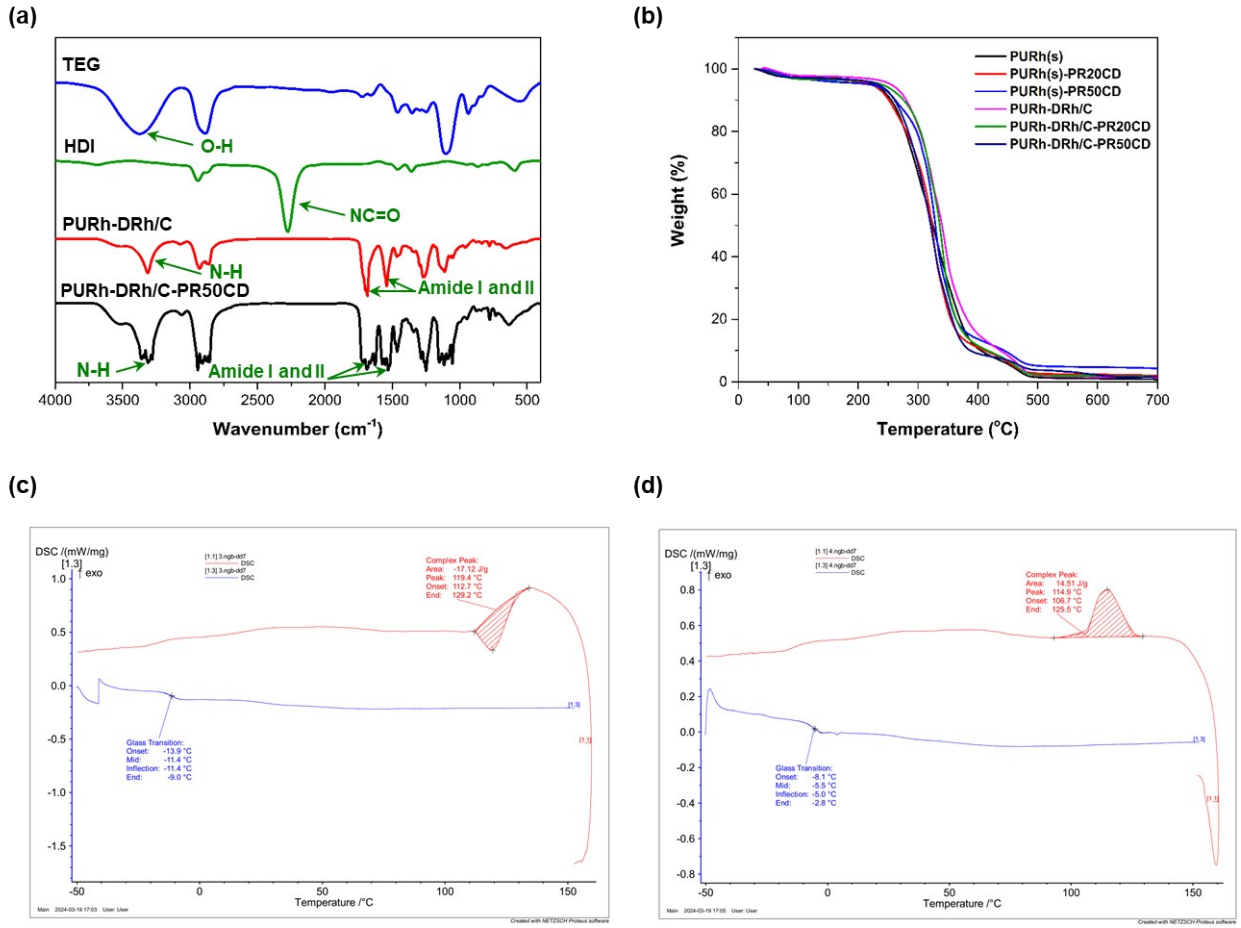

Fig. S1 (a) FTIR spectra of TEG, HDI, **PURh-DRh/C** and **PURh-DRh/C-PR50CD**. (b) TGA curves of different PU films. (c) and (d) DSC profiles (at a heating/cooling rate of 10 °C/min) of **PURh-DRh/C-PR50CD** film before and after stretching (ca. 7000% strain).

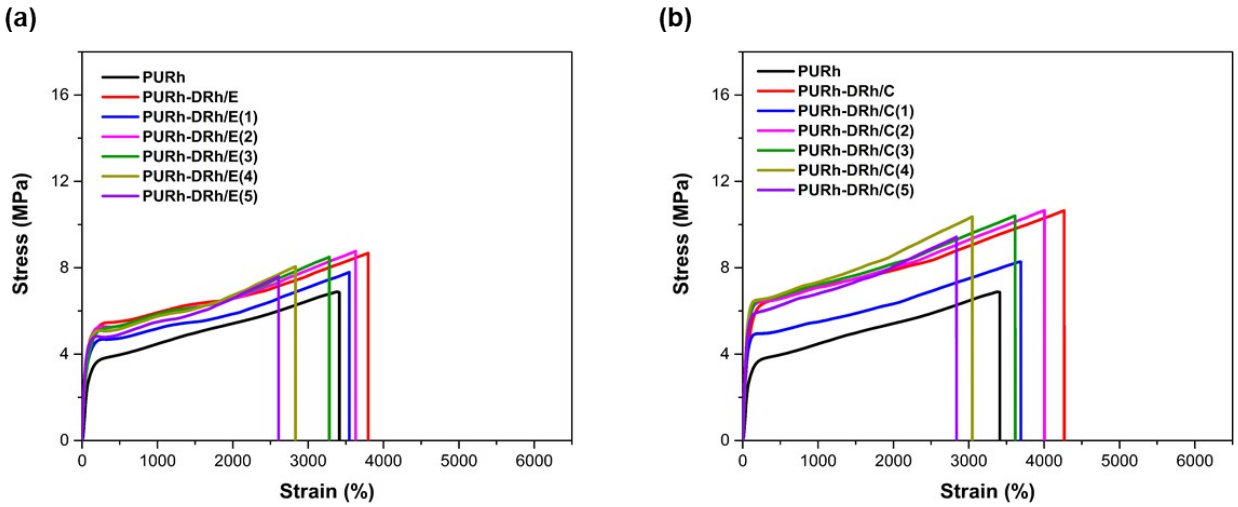

Fig. S2 Stress-strain curves of (a) **PURh-DRh/E** and (b) **PURh-DRh/C** films (strain rate of 1 mm/s) with different percentages of implanted daisy chain rotaxanes **DRh/E** and **DRh/C**.

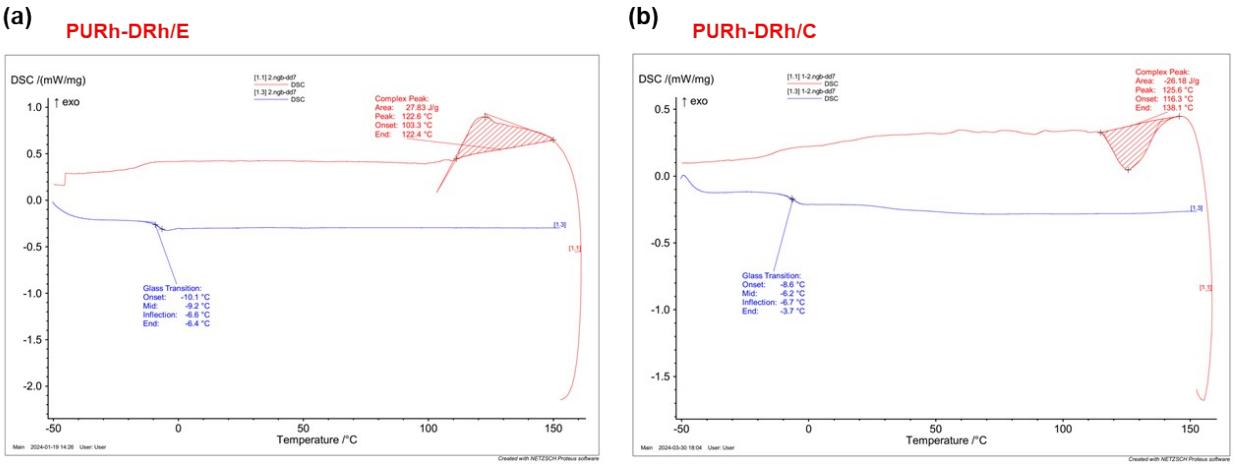

Fig. S3 DSC profiles of (a) **PURh-DRh/E** and (b) **PURh-DRh/C** films (at a heating/cooling rate of 10 °C/min).

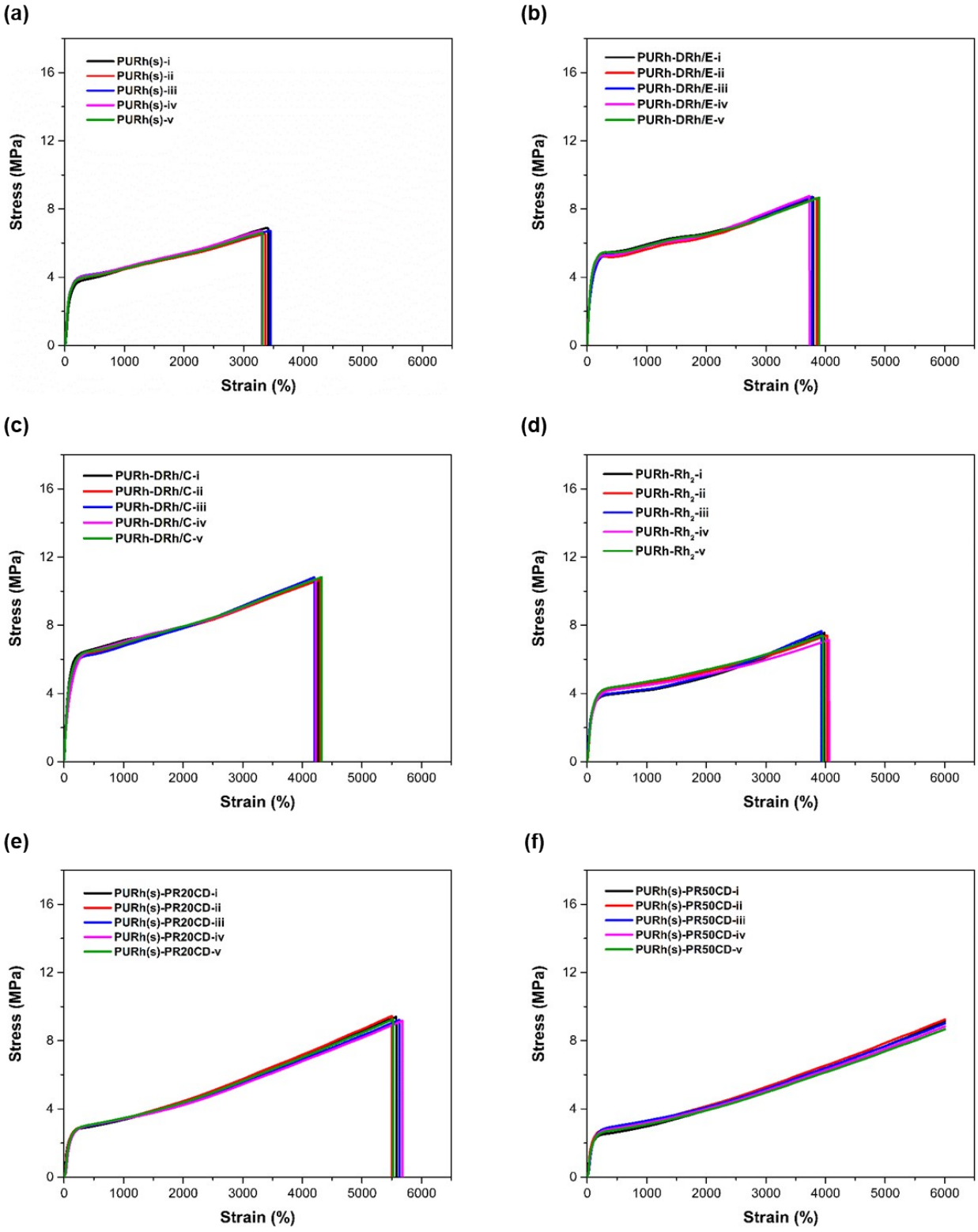

Fig. S4 Stress-strain curves of (a) **PURh(s)**, (b) **PURh-DRh/E**, (c) **PURh-DRh/C**, (d) **PURh-Rh$_2$**, (e) **PURh(s)-PR20CD** and (f) **PURh(s)-PR50CD** films (at a strain rate of 1 mm/s) with 5 batches (denoted as i-v) of the same PU samples.

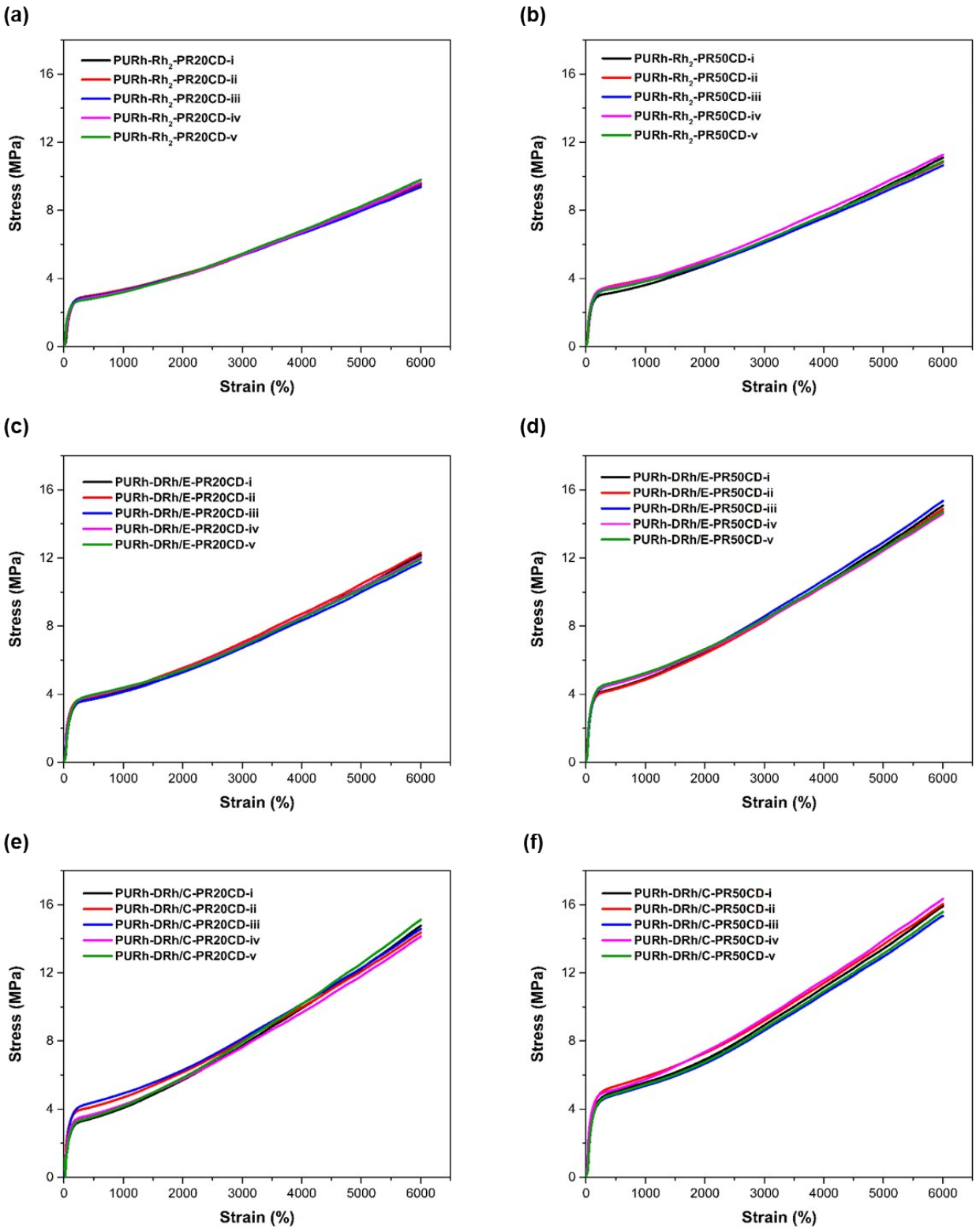

Fig. S5 Stress-strain curves of (a) **PURh-Rh$_2$-PR20CD**, (b) **PURh-Rh$_2$-PR50CD**, (c) **PURh-DRh/E-PR20CD**, (d) **PURh-DRh/E-PR50CD**, (e) **PURh-DRh/C-PR20CD** and (f) **PURh-DRh/C-PR50CD** films (at a strain rate of 1 mm/s) with 5 batches (denoted as i-v) of the same PU samples.

Table S1 Mechanical properties of PU (including the optimized **PURh-DRh/E**) films based on various molar amounts of **DRh/E**

PU Samples[a]	**Rh** (mmol)	**TEG** (mmol)	**HDI** (mmol)	**TEA** (mmol)	**DRh/E** (mmol)	Breaking Stress (MPa)	Breaking Strain (%)
PURh(s)	0.0500	4.45	6.0	0.25	0	6.85	3414 ± 71
PURh-DRh/E(1)	0.0475	4.45	6.0	0.25	0.00125	7.80	3547 ± 69
PURh-DRh/E*	0.0450	4.45	6.0	0.25	0.00250	8.68	3797 ± 78
PURh-DRh/E(2)	0.0425	4.45	6.0	0.25	0.00375	8.77	3632 ± 75
PURh-DRh/E(3)	0.0400	4.45	6.0	0.25	0.00500	8.50	3282 ± 60
PURh-DRh/E(4)	0.0375	4.45	6.0	0.25	0.00625	8.06	2832 ± 53
PURh-DRh/E(5)	0.0350	4.45	6.0	0.25	0.00750	7.59	2609 ± 51

[a] The total molar numbers of mechano-fluorophoric rhodamine moieties for **Rh** and **DRh/E** were maintained as 0.05 mmol in all PU films.

* The optimized composition of **PURh-DRh/E** with the best mechanical property based on various molar amounts of **DRh/E**.

Table S2 Mechanical properties of PU (including the optimized **PURh-DRh/C**) films based on various molar amounts of **DRh/C**

PU Samples[a]	**Rh** (mmol)	**TEG** (mmol)	**HDI** (mmol)	**TEA** (mmol)	**DRh/C** (mmol)	Breaking Stress (MPa)	Breaking Strain (%)
PURh(s)	0.0500	4.45	6.0	0.25	0	6.85	3414 ± 71
PURh-DRh/C(1)	0.0475	4.45	6.0	0.25	0.00125	8.28	3691 ± 68
PURh-DRh/C*	0.0450	4.45	6.0	0.25	0.00250	10.65	4267 ± 75
PURh-DRh/C(2)	0.0425	4.45	6.0	0.25	0.00375	10.66	4005 ± 81
PURh-DRh/C(3)	0.0400	4.45	6.0	0.25	0.00500	10.41	3616 ± 76
PURh-DRh/C(4)	0.0375	4.45	6.0	0.25	0.00625	10.36	3048 ± 54
PURh-DRh/C(5)	0.0350	4.45	6.0	0.25	0.00750	9.43	2837 ± 48

[a] The total molar numbers of mechano-fluorophoric rhodamine moieties for **Rh** and **DRh/C** were maintained as 0.05 mmol in all PU films.

* The optimized composition of **PURh-DRh/C** with the best mechanical property based on various molar amounts of **DRh/C**.

Table S3 Mechanical properties of **PURh-Rh$_2$** films with different cross-linkers

PU Samples[a]	**Rh** (mmol)	**TEG** (mmol)	**HDI** (mmol)	**TEA** (mmol)	**Rh$_2$** (mmol)	**PR20CD**	**PR50CD**	Breaking Stress (MPa)	Breaking Strain (%)
PURh(s)	0.050	4.45	6.0	0.25	0	0	0	6.85	3414 ± 71
PURh-Rh$_2$	0.045	4.45	6.0	0.25	0.0025	0	0	7.56	3985 ± 82
PURh-Rh$_2$-PR20CD	0.045	4.45	6.0	0	0.0025	1 wt%	0	> 9.57	> 6000
PURh-Rh$_2$-PR50CD	0.045	4.45	6.0	0	0.0025	0	1 wt%	> 11.10	> 6000

[a] The total molar numbers of mechano-fluorophoric rhodamine moieties for **Rh** and **Rh$_2$** were maintained as 0.05 mmol in all PU films.

Table S4 Mechanical properties of **PURh(s)** films with different cross-linkers

PU Samples	**Rh** (mmol)	**TEG** (mmol)	**HDI** (mmol)	**TEA** (mmol)	**PR20CD**	**PR50CD**	Breaking Stress (MPa)	Breaking Strain (%)
PURh(s)	0.05	4.45	6.0	0.25	0	0	6.85	3414 ± 71
PURh(s)-PR20CD	0.05	4.45	6.0	0	1 wt%	0	9.19	5579 ± 104
PURh(s)-PR50CD	0.05	4.45	6.0	0	0	1 wt%	> 9.14	> 6000

Table S5 Mechanical properties of **PURh-DRh/E** films with different cross-linkers

PU Samples	**Rh** (mmol)	**TEG** (mmol)	**HDI** (mmol)	**TEA** (mmol)	**DRh/E** (mmol)	**PR20CD**	**PR50CD**	Breaking Stress (MPa)	Breaking Strain (%)
PURh-DRh/E	0.045	4.45	6.0	0.25	0.0025	0	0	8.68	3797 ± 78
PURh-DRh/E-PR20CD	0.045	4.45	6.0	0	0.0025	1 wt%	0	> 12.19	> 6000
PURh-DRh/E-PR50CD	0.045	4.45	6.0	0	0.0025	0	1 wt%	> 15.07	> 6000

Table S6 Mechanical properties of **PURh-DRh/C** films with different cross-linkers

PU Samples	**Rh** (mmol)	**TEG** (mmol)	**HDI** (mmol)	**TEA** (mmol)	**DRh/C** (mmol)	**PR20CD**	**PR50CD**	Breaking Stress (MPa)	Breaking Strain (%)
PURh-DRh/C	0.045	4.45	6.0	0.25	0.0025	0	0	10.65	4267 ± 75
PURh-DRh/C-PR20CD	0.045	4.45	6.0	0	0.0025	1 wt%	0	> 14.77	> 6000
PURh-DRh/C-PR50CD	0.045	4.45	6.0	0	0.0025	0	1 wt%	> 15.93	> 6000

Table S7 Young's moduli of PU films with different monomer components

PU Samples	Young's Modulus (MPa)	PU Samples	Young's Modulus (MPa)
PURh(s)	4.79 ± 0.10	**PURh-Rh_2-PR20CD**	3.67 ± 0.09
PURh-Rh_2	5.16 ± 0.11	**PURh-Rh_2-PR50CD**	3.58 ± 0.08
PURh-DRh/E	6.72 ± 0.14	**PURh-DRh/E-PR20CD**	4.35 ± 0.10
PURh-DRh/C	7.79 ± 0.17	**PURh-DRh/E-PR50CD**	4.16 ± 0.09
PURh(s)-PR20CD	3.47 ± 0.08	**PURh-DRh/C-PR20CD**	5.73 ± 0.13
PURh(s)-PR50CD	3.37 ± 0.07	**PURh-DRh/C-PR50CD**	5.57 ± 0.12

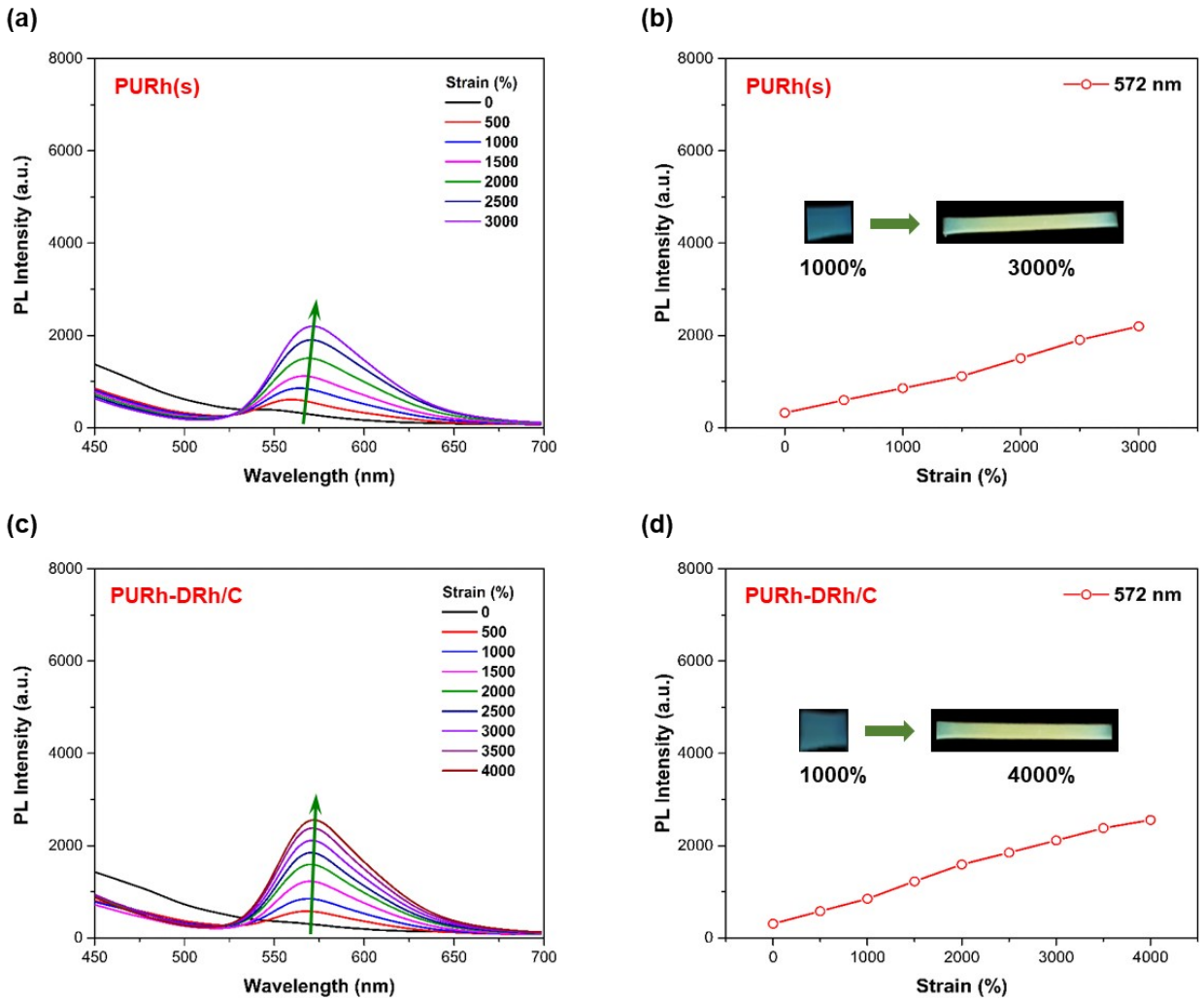

Fig. S6 (a), (c) PL spectra and (b), (d) relative PL intensities of yellow-orange-emissive rhodamine (λ_{em} = 572 nm) for **PURh(s)** and **PURh-DRh/C** films with different strains (λ_{ex} = 365 nm).

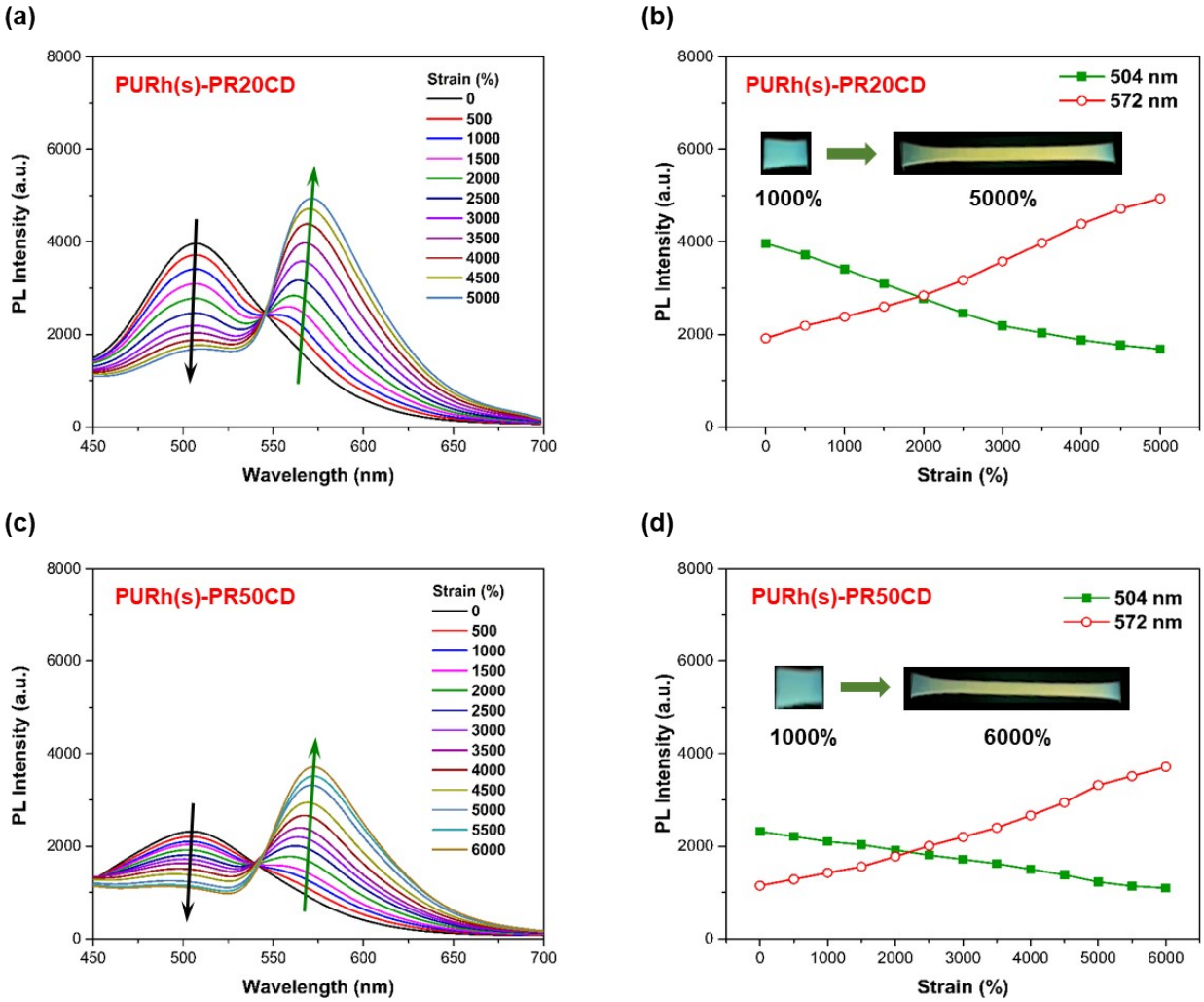

Fig. S7 (a), (c) PL spectra and (b), (d) relative PL intensities of green-emissive naphthalimide (λ_{em} = 504 nm) and yellow-orange-emissive rhodamine (λ_{em} = 572 nm) for **PURh(s)-PR20CD** and **PURh(s)-PR50CD** films with different strains (λ_{ex} = 365 nm).

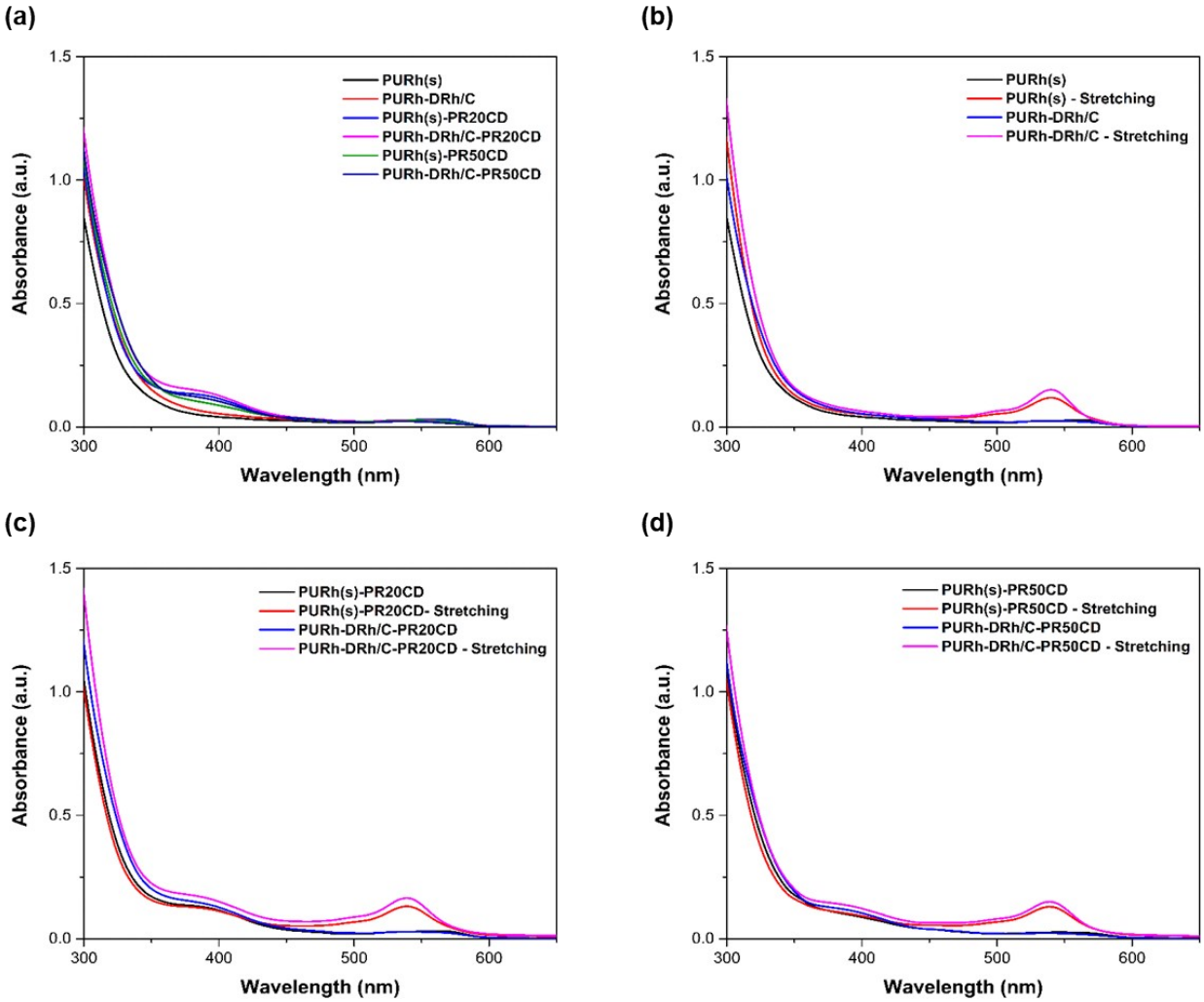

Fig. S8 (a) UV-vis spectra of different PU films. UV-vis spectra of (b) **PURh(s)** and **PURh-DRh/C**, (c) **PURh(s)-PR20CD** and **PURh-DRh/C-PR20CD** and (d) **PURh(s)-PR50CD** and **PURh-DRh/C-PR50CD** before and after stretching.

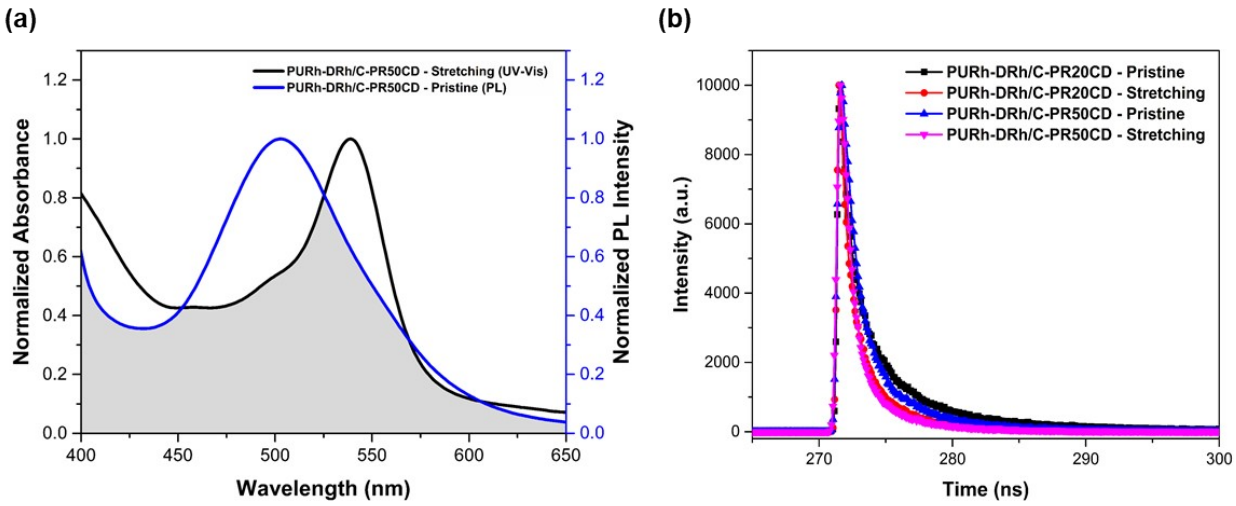

Fig. S9 (a) Spectral overlap between the emission spectrum of pristine **PURh-DRh/C-PR50CD** film and absorption spectrum of stretched **PURh-DRh/C-PR50CD** film (λ_{ex} = 365 nm). (b) TRPL profiles of **PURh-DRh/C-PR20CD** and **PURh-DRh/C-PR50CD** films before and after stretching (λ_{ex} = 375 nm, λ_{em} = 504 nm).

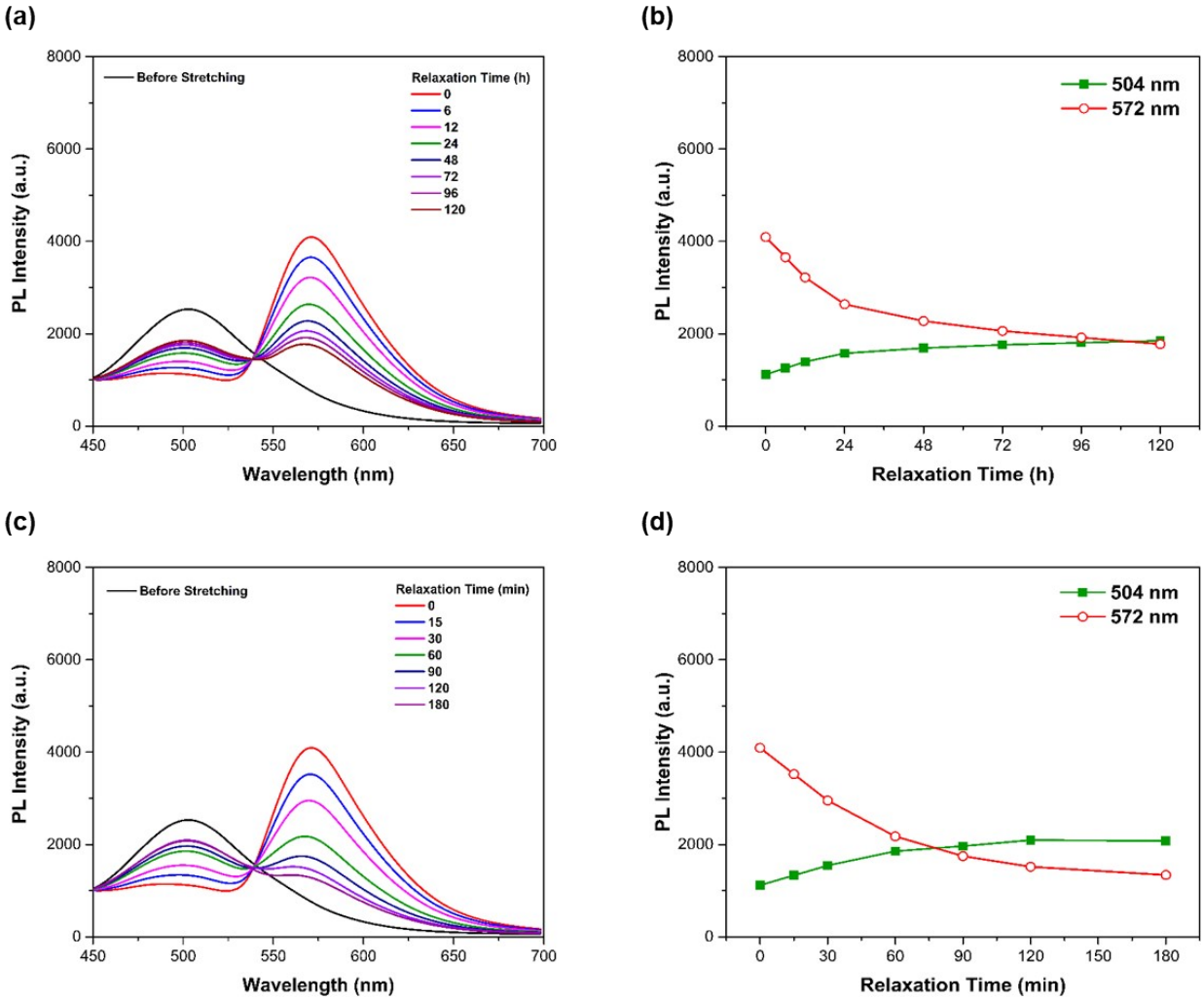

Fig. S10 PL spectra and relative PL intensities of green-emissive naphthalimide (λ_{em} = 504 nm) and yellow-orange-emissive rhodamine (λ_{em} = 572 nm) for **PURh-DRh/C-PR50CD** films with different relaxation time after fracture (a), (b) at room temperature and (c), (d) upon heating at 100 °C.

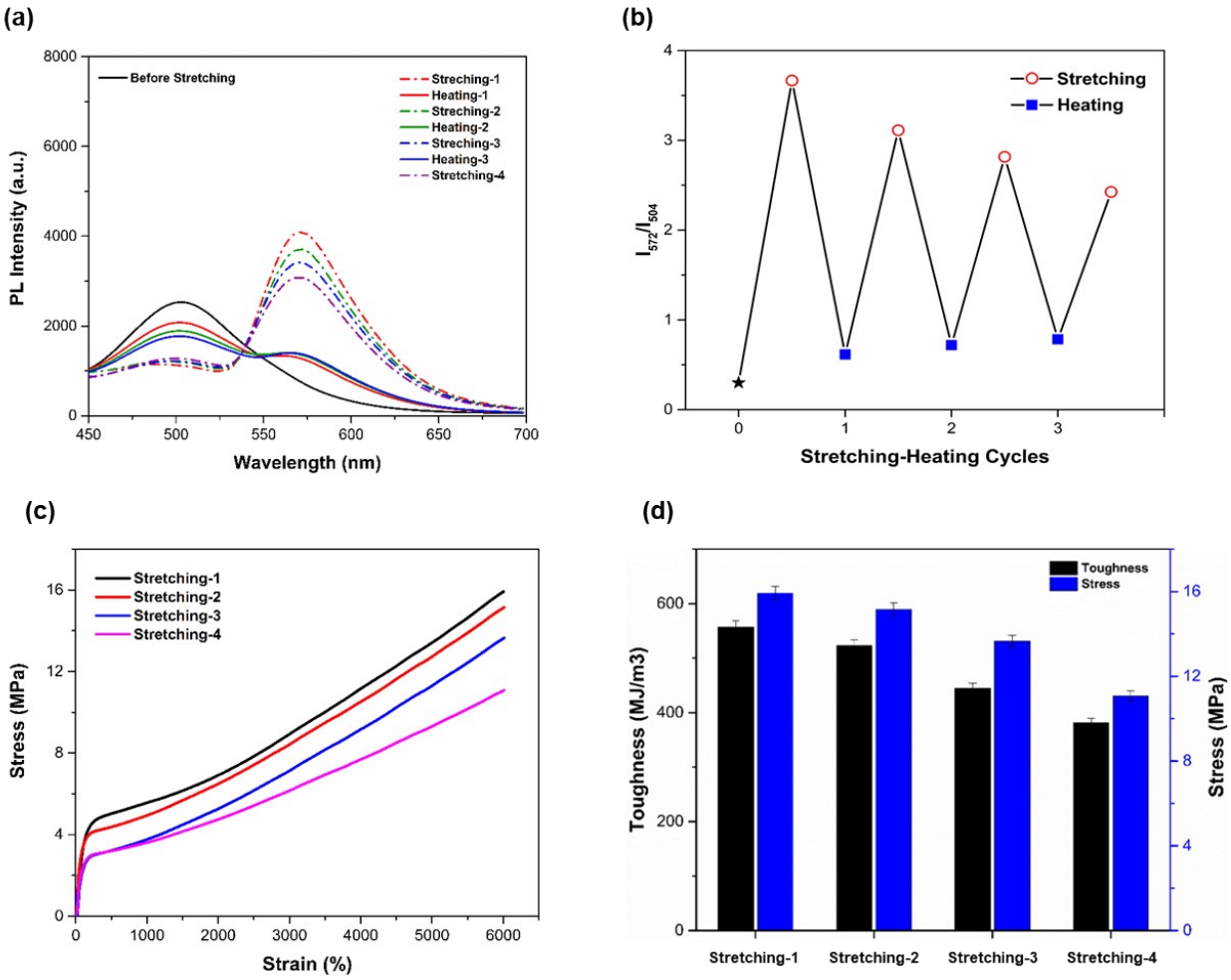

Fig. S11 (a) PL spectra and (b) PL intensity ratios of two emission bands at 504 and 572 nm for **PURh-DRh/C-PR50CD** film by 3 cycles of stretching and thermal treatments (heating at 100 °C) (λ_{ex} = 365 nm). (c) Stress-strain curves and (d) toughness/stress histograms of **PURh-DRh/C-PR50CD** film (strain rate of 1 mm/s) under 3 stretching-heating cycles.

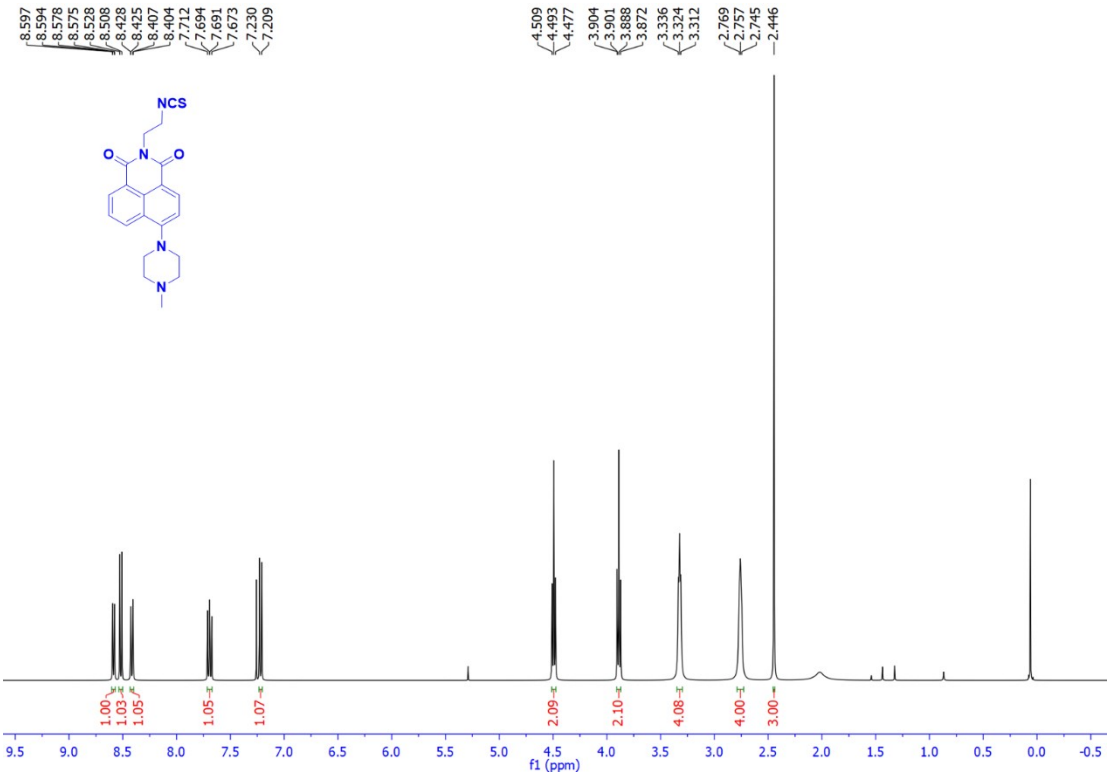

Fig. S12 ^{1}H NMR spectrum (400 MHz, $CDCl_3$) of compound **Nap-NCS**.

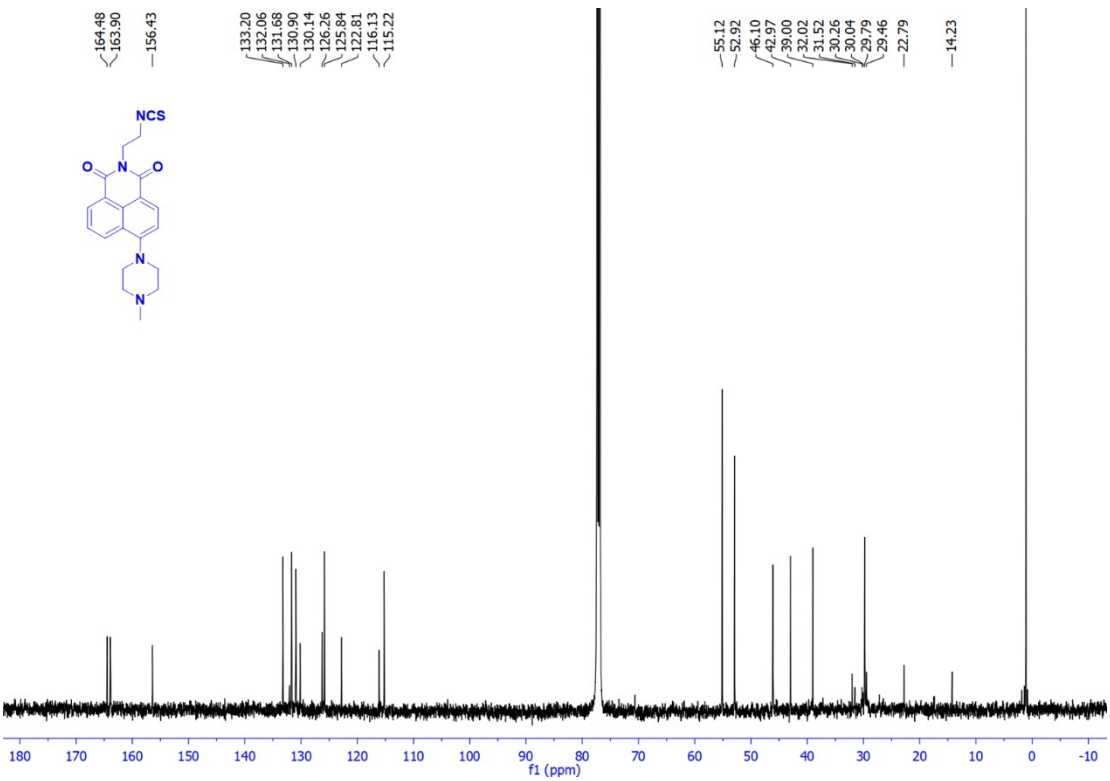

Fig. S13 ^{13}C NMR spectrum (125 MHz, $CDCl_3$) of compound **Nap-NCS**.

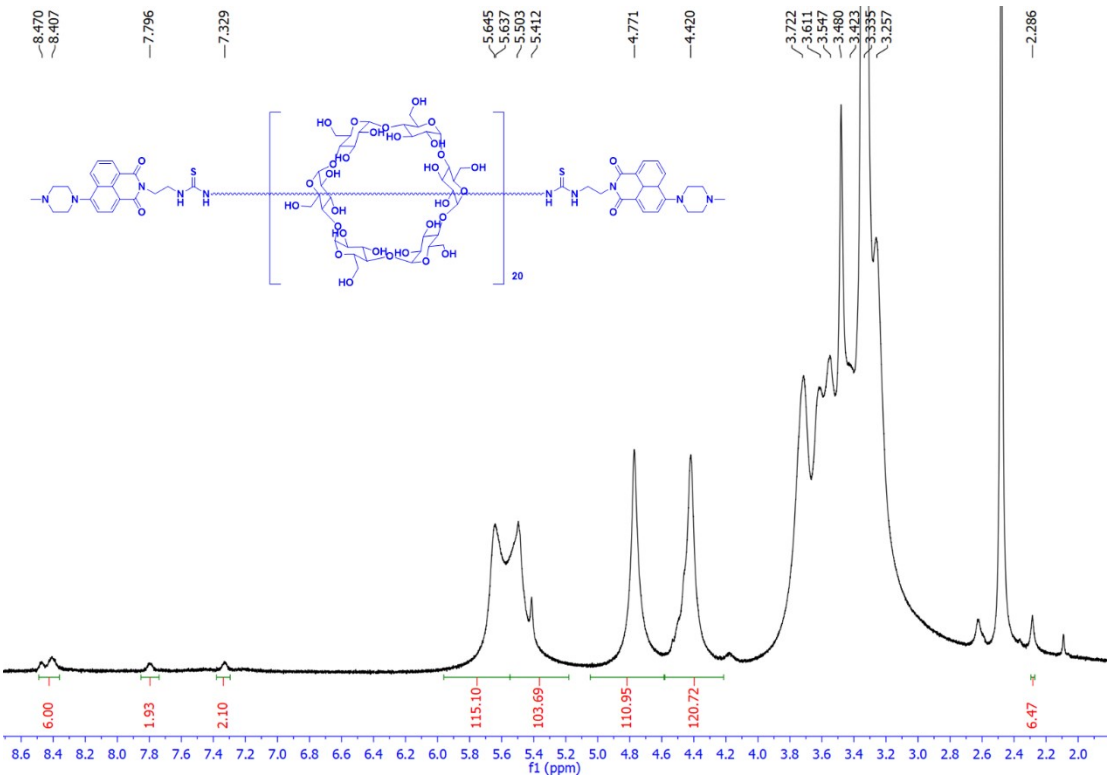

Fig. S14 ^{1}H NMR spectrum (600 MHz, DMSO-d_6) of compound **PR20CD**.

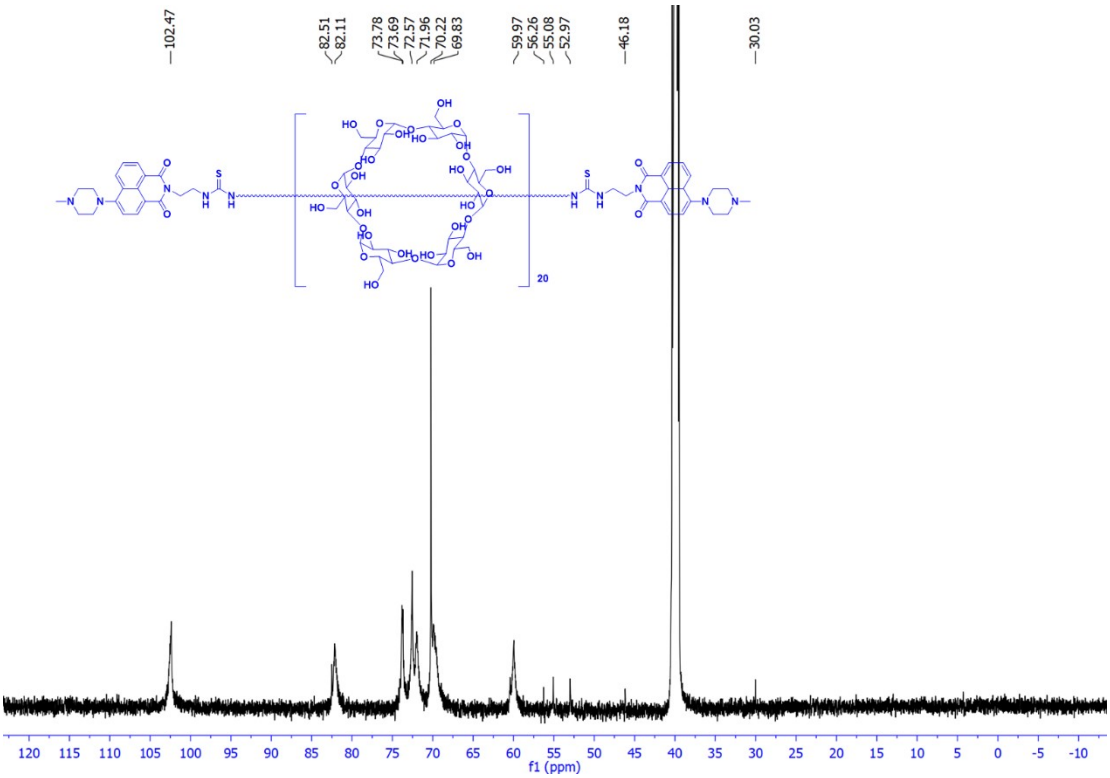

Fig. S15 ^{13}C NMR spectrum (150 MHz, DMSO-d_6) of compound **PR20CD**.

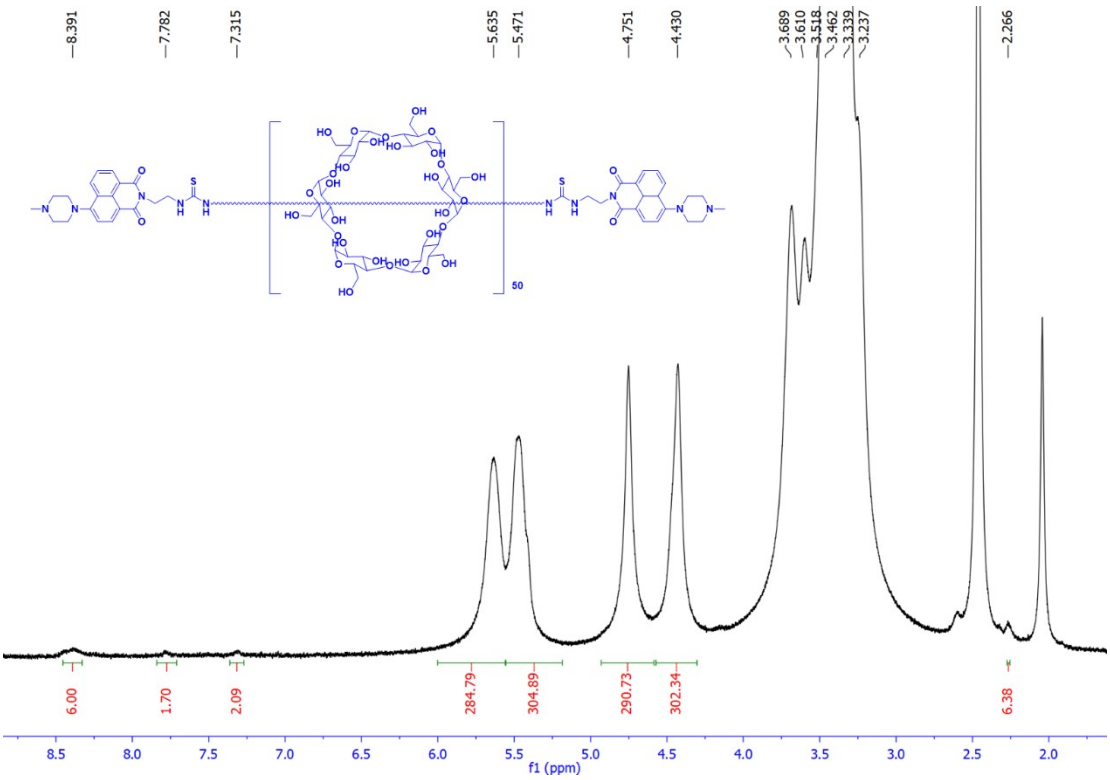

Fig. S16 ^{1}H NMR spectrum (600 MHz, DMSO-d_6) of compound **PR50CD**.

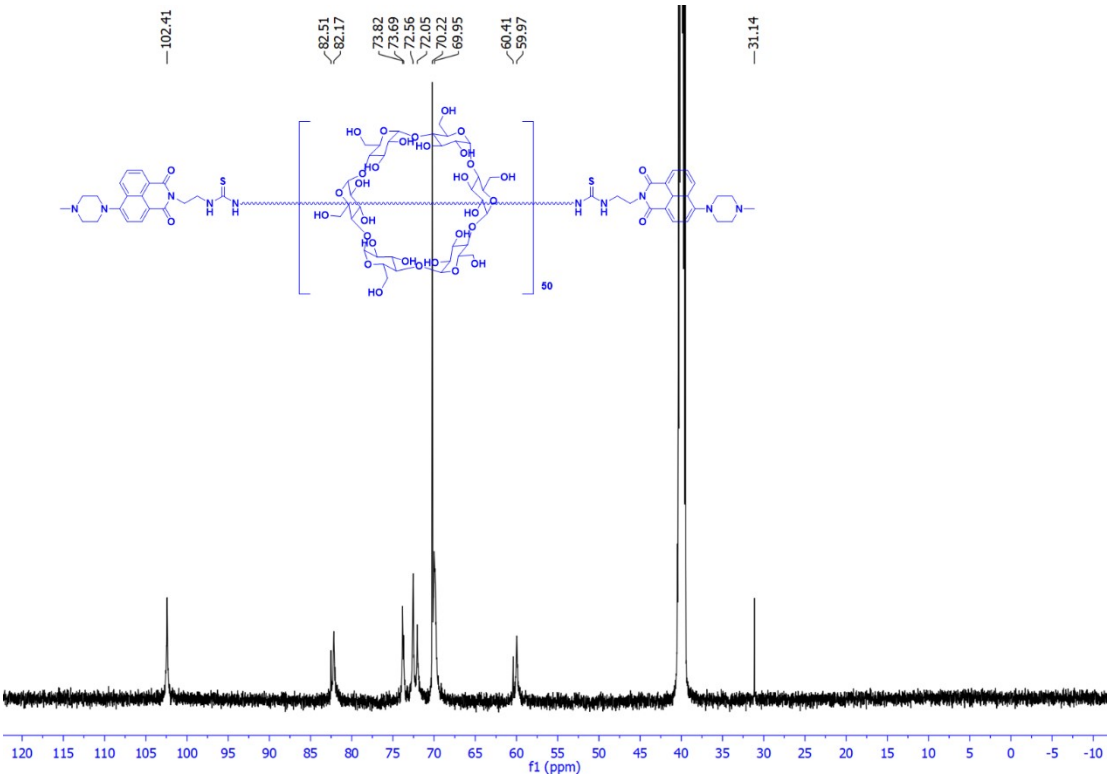

Fig. S17 ^{13}C NMR spectrum (150 MHz, DMSO-d_6) of compound **PR50CD**.

References

S1 Z. Wang, Z. Ma, Y. Wang, Z. Xu, Y. Luo, Y. Wei and X. Jia, *Adv. Mater.*, 2015, **27**, 6469-6474.

S2 T. T. K. Cuc, P. Q. Nhien, T. M. Khang, C.-C. Weng, C.-H. Wu, B.-t. B. Hue, Y.-K. Li, J. I. Wu and H.-C. Lin, *Chem. Mater.*, 2020, **32**, 9371-9389.

S3 T. T. K. Cuc, C.-H. Hung, T.-C. Wu, P. Q. Nhien, T. M. Khang, B. T. B. Hue, W.-T. Chuang and H.-C. Lin, *Chem. Eng. J.*, 2024, **485**, 149694.

S4 T. M. Khang, R. Huang, A. Khan, W.-T. Chuang, P. Q. Nhien, T. T. K. Cuc, B. T. B. Hue, K.-H. Wei, Y.-K. Li and H.-C. Lin, *ACS Materials Lett.*, 2022, **4**, 2537-2546.

S5 T. T. K. Cuc, P. Q. Nhien, T. M. Khang, H.-Y. Chen, C.-H. Wu, B.-t. B. Hue, Y.-K. Li, J. I. Wu and H.-C. Lin, *ACS Appl. Mater. Interfaces*, 2021, **13**, 20662-20680.